An Investigation of Nonreciprocal Periodic Structures

TERRY A. ENEGREN AND M. M. Z. KHARADLY

Abstract—**The properties of a nonreciprocal ferrite-loaded rectangular waveguide, which is periodically loaded by thin metallic "inductive" diaphragms, are investigated experimentally. The propagation constants of the structure are measured and are compared with predictions based on measured values of the scattering parameters of a single diaphragm in the nonreciprocal waveguide. The agreement between theory and experiment is generally good except for the smaller spacings between the loading diaphragms. This discrepancy is attributed to the effects of higher order mode interaction.**

I. Introduction

RECIPROCAL periodic structures have been the subject of extensive investigation because they have a variety of important practical applications. Recently, a comprehensive review of the subject has been made by Elachi [1].

Various methods exist for the analysis of these structures depending on the nature of the loading. If the periodic nature of the medium can be easily incorporated into the wave equation, then solutions involving Hill functions are appropriate. In cases such as corrugated surfaces or tape helices, analysis by expansion of the fields into Floquet harmonics is more convenient, however. The conventional transmission line approach is appropriate when the periodic loading is accomplished through regular placement of obstacles. This requires knowledge of the scattering parameters of the obstacle and the propagation characteristics of the unloaded line.

Nonreciprocal waveguides have the property that their propagation characteristics are dependent on the direction of propagation. This property has been exploited in many applications, of which the nonreciprocal ferrite phase shifter is an example of current interest. In this particular case, it is desirable to enhance the nonreciprocal effect and it has been shown that this can be easily achieved through periodic loading of the nonreciprocal medium [2], [3].

To date, little has been done on the subject of nonreciprocal periodic structures. The geometry of the structure and the complicated form of the wave equation in anisotropic media often make the direct analytical techniques, mentioned above, difficult to apply. But for periodic loading by discrete obstacles, the transmission line approach [4] has been used with comparative ease. In this approach, the nonreciprocal medium is represented by a transmission line having different propagation constants for the two directions of propagation. The discontinuity is represented by a nonreciprocal two-port junction which may then be used to derive an equivalent circuit whose elements have two sets of values, one for each direction of propagation. The evaluation of the nonreciprocal equivalent circuits has been done for particular configurations of discontinuities within nonreciprocal waveguides [5]. The scattering parameters of particular configurations of the interface between reciprocal and nonreciprocal waveguides have also been evaluated [6], [7].

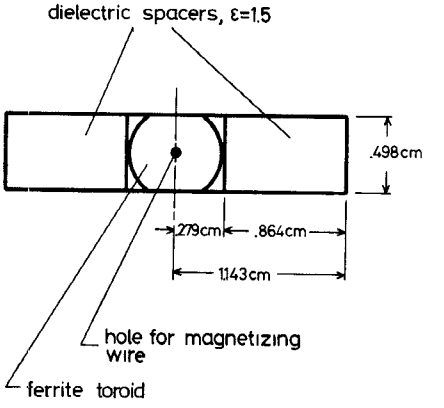

Fig. 1. Cross section of experimental configuration.

In this paper the properties of nonreciprocal periodic structures are investigated experimentally. The nonreciprocal medium consists of a rectangular waveguide symmetrically loaded by a transversely magnetized ferrite toroid as shown in Fig. 1. Only the dominant modes propagate. Periodic loading is accomplished through regular placement of thin metallic "inductive" diaphragms.

The main points of this investigation are:

a) measurement of the nonreciprocal equivalent circuit of a thin metallic diaphragm;
b) direct measurement of fields in the nonreciprocal waveguide; and
c) application of the transmission line approach to nonreciprocal periodic structures.

Manuscript received July 10, 1979; revised April 1, 1980. This work was supported by the Natural Sciences and Engineering Research Council of Canada under Grant A-3344.

T. A. Enegren was with Department of Electrical Engineering, The University of British Columbia, Vancouver, B.C., Canada. He is now with the MPB Technologies, Inc., P.O. Box 160, 21051 North Service Road, Ste-Anne-de-Bellevue, Quebec, Canada H9X 3L5.

M. M. Z. Kharadly is with Department of Electrical Engineering, The University of British Columbia, Vancouver, B.C., Canada.

0018-9480/80/0800-0905$00.75 ©1980 IEEE

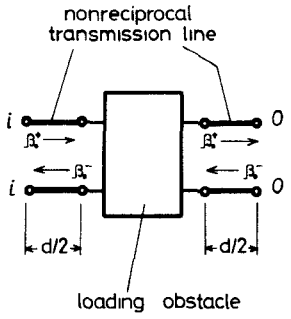

Fig. 2. Nonreciprocal two-port junction representation for unit cell of periodic structure with spacing d.

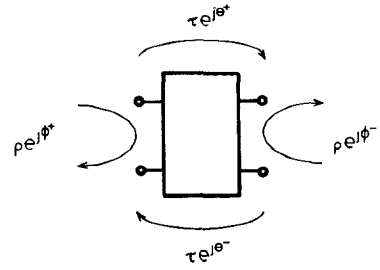

Fig. 3. Nonreciprocal two-port junction representation for loading obstacle.

II. Wave Matrix Analysis of Nonreciprocal Periodic Structure

A. Propagation Constants

The analysis presented here is similar to that in [4]. However, using the unitary conditions for the scattering matrix of the loading obstacle, a relatively simple eigenvalue equation can be derived. The basic unit cell of a nonreciprocal transmission line periodically loaded with discrete loading obstacles, may be represented as shown in Fig. 2. The loading obstacle may be represented by a two port junction whose reflection and transmission coefficients are defined in Fig. 3 and its wave amplitude transmission matrix is thus given by

$$\begin{bmatrix} \frac{1}{\tau}\exp(-j\theta^+) & -\frac{\rho}{\tau}\exp[j(\phi^- - \theta^+)] \\ \frac{\rho}{\tau}\exp[j(\phi^+ - \theta^+)] & \frac{1}{\tau}\exp(j\theta^-) \end{bmatrix} \quad (1)$$

where

$$\rho^2+\tau^2=1$$
$$\phi^+ + \phi^- - \theta^+ - \theta^- = \pm 180°. \quad (2)$$

The wave amplitude transmission matrix for the nonreciprocal section of transmission line is given by

$$\begin{bmatrix} \exp(j\beta_0^+ d/2) & 0 \\ 0 & \exp(-j\beta_0^- d/2) \end{bmatrix}. \quad (3)$$

The positive and negative superscripts denote propagation in forward and backward directions, respectively. Thus the overall matrix for the unit cell is

$$A=\begin{bmatrix} \frac{1}{\tau}\exp[-j(\theta^+ - \psi^+)] & -\frac{\rho}{\tau}\exp\left[j\left(\phi^- + \frac{\psi^+ - \psi^-}{2} - \theta^+\right)\right] \\ \frac{\rho}{\tau}\exp\left[j\left(\phi^+ + \frac{\psi^+ - \psi^-}{2} - \theta^+\right)\right] & \frac{1}{\tau}\exp[j(\theta^- - \psi^-)] \end{bmatrix} \quad (4)$$

where

$$\psi^+ = \beta_0^+ d$$
$$\psi^- = \beta_0^- d. \quad (5)$$

The solution for Bloch waves requires

$$\det(A - \exp(\gamma d) I) = 0 \quad (6)$$

where I is the unit matrix and γ is the propagation coefficient for the forward propagating Bloch wave. Condition (6) yields the following eigenvalue equation:

$$\cosh\left(\gamma d + j\frac{\delta}{2}\right) = \frac{1}{\tau}\cos\left(\frac{\Omega^+ + \Omega^-}{2}\right) \quad (7)$$

where

$$\Omega^+ = \theta^+ - \psi^+$$
$$\Omega^- = \theta^- - \psi^-$$
$$\delta = \Omega^+ - \Omega^- \quad (8)$$

For propagating waves, $\gamma = j\beta$. The two solutions β^+ and β^- for forward and backward propagating Bloch waves are given by

$$\beta^+ = \left\{-\frac{\delta}{2} + \cos^{-1}\left(\frac{1}{\tau}\cos\frac{(\Omega^+ + \Omega^-)}{2}\right)\right\} \Big/ d$$
$$\beta^- = \left\{\frac{\delta}{2} + \cos^{-1}\left(\frac{1}{\tau}\cos\frac{(\Omega^+ + \Omega^-)}{2}\right)\right\} \Big/ d. \quad (9)$$

Thus the difference in the propagation constants is given by

$$\Delta\beta = \beta^- - \beta^+ = \delta/d. \quad (10)$$

Substituting from (5) and (8) into (10) yields

$$\Delta\beta = \Delta\beta_0 + (\theta^+ - \theta^-)/d$$

where $\Delta\beta_0$ is the difference in the propagation constants of the unloaded line

$$\Delta\beta_0 = \beta_0^- - \beta_0^+.$$

For $\beta_0^- > \beta_0^+$ the quantity $[\theta^+ - \theta^-]$ is positive for "inductive" loading and hence the difference in the propagation constants is increased.

B. Bloch-Wave Impedance

The Bloch-wave impedance is defined as the impedance necessary to terminate a periodic structure such that there is no reflected Bloch wave. The Bloch-wave impedance is not unique but depends on the choice of terminal planes. Refering to Fig. 2, let the unit cell be matched by connect-

ing an impedance Z_B^+ to terminals *o-o*. Z_B^+ is then equal to the input impedance seen at terminals *i-i*. Similarily the input impedance at terminals *o-o* yields Z_B^- when the unit cell is terminated by Z_B^- at terminals *i-i*. The Bloch-wave impedances are usually normalized to the characteristic impedances of the unloaded nonreciprocal transmission line $Z_c^{\pm}$. It has been shown theoretically for the twin-slab configuration of magnetized ferrite [7], and experimentally in this work, that Z_c^+ is almost exactly equal to Z_c^-. Hence, for practical purposes, it is justifiable to set $Z_c^+ = Z_c^- = 1$.

The wave matrix for the unit cell A can decomposed as follows:

$$A = PDP^{-1}. \tag{11}$$

The matrix D is a diagonal matrix whose elements are the eigenvalues of A

$$D = \begin{bmatrix} \exp(j\beta^+ d) & 0 \\ 0 & \exp(-j\beta^- d) \end{bmatrix} \tag{12}$$

where β^+ and β^- are the propagation coefficients for the forward and backward propagating Bloch waves. The columns of the matrix P are the eigenvectors of A. The matrix P can be written as

$$P = \frac{1}{2(U^+ + U^-)} \begin{bmatrix} U^+ + 1 & U^- - 1 \\ U^+ - 1 & U^- + 1 \end{bmatrix} \tag{13}$$

where

$$U^+ = \frac{A_{12} - \frac{A_{11} - A_{22}}{2} + \S}{\frac{A_{11} - A_{22}}{2} - \S + A_{12}}$$

$$U^- = \frac{A_{21} + \frac{A_{11} - A_{22}}{2} - \S}{A_{21} - \frac{A_{11} - A_{22}}{2} + \S}$$

and

$$\S = \sqrt{\frac{(A_{11} + A_{22})^2}{2} + (A_{11}A_{22} - A_{12}A_{21})} \tag{14}$$

where A_{ij} are the elements of the matrix A.

The unit cell is equivalent to the network shown in Fig. 4. The nonreciprocal section of transmission line of length d supports the Bloch waves. The matrices P and P^{-1} can be interpreted as describing the interface effects between this section and the unloaded nonreciprocal transmission line. Let the matching impedance Z_B^+ be connected to the terminals *o-o*. The input impedance at the terminals *i-i* can be found by connecting these terminals to the unloaded line. An incident wave excites a forward propagating Bloch wave. Since a reflected Bloch wave is not produced, the reflection coefficient R at the terminals *i-i* can be calculated from the wave matrix P

$$R = \frac{P_{21}}{P_{11}} = \frac{U^+ - 1}{U^+ + 1}. \tag{15}$$

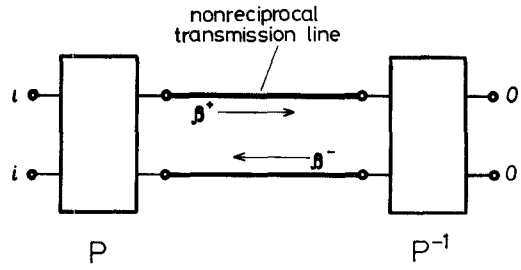

Fig. 4. Equivalent representation for unit cell.

Hence the Bloch-wave impedance Z_B^+ is given by

$$Z_B^+ = \frac{1 - R}{1 + R} = U^+. \tag{16}$$

Following a similar procedure for Z_B^- yields

$$Z_B^- = U^-. \tag{17}$$

III. Experiment

The main objectives of the experimental investigation are (1) to measure the scattering parameters of a thin inductive diaphragm in a nonreciprocal waveguide and (2) to measure the propagation constants of a nonreciprocal periodic structure.

Measurement of the diaphragm in a nonreciprocal section of waveguide requires accounting for the effects of the interfaces between the reciprocal and nonreciprocal waveguides. One approach is to measure the properties of the interface and then account for them in the diaphragm measurements. The application of this approach has resulted in considerable error in the scattering parameters for the diaphragm. In this paper another approach is taken where the interfaces are matched thus allowing the scattering parameters of the diaphragm to be directly obtained through measurement of the reflection and transmission coefficients, as discussed in Section III-C. This is made experimentally feasible through the use of a specially-constructed waveguide section that permitted direct sampling of the electric field along the nonreciprocal waveguide. This arrangement also allowed easy and accurate determination of the propagation characteristics of the nonreciprocal periodic structures.

A. The Measurement Section

A photograph of the measurement section is shown in Fig. 5. The central part accommodates the ferrite toroids and the linear tapers provide a gradual transition to standard X-band waveguide. The maximum VSWR produced by the tapers at the frequencies at which measurements were taken was 0.2 dB. The ferrite toroid was centered by dielectric spacers of relative permittivity $\epsilon_r = 1.5$. The transverse symmetry ensured that only the dominant modes propagated. The length of the ferrite rod was 4.57 cm. The ferrite was magnetized to saturation by passing 15 A, through a magnetization wire. To eliminate errors due to the magnetization wire, the ferrite was magnetized externally and then placed into the block

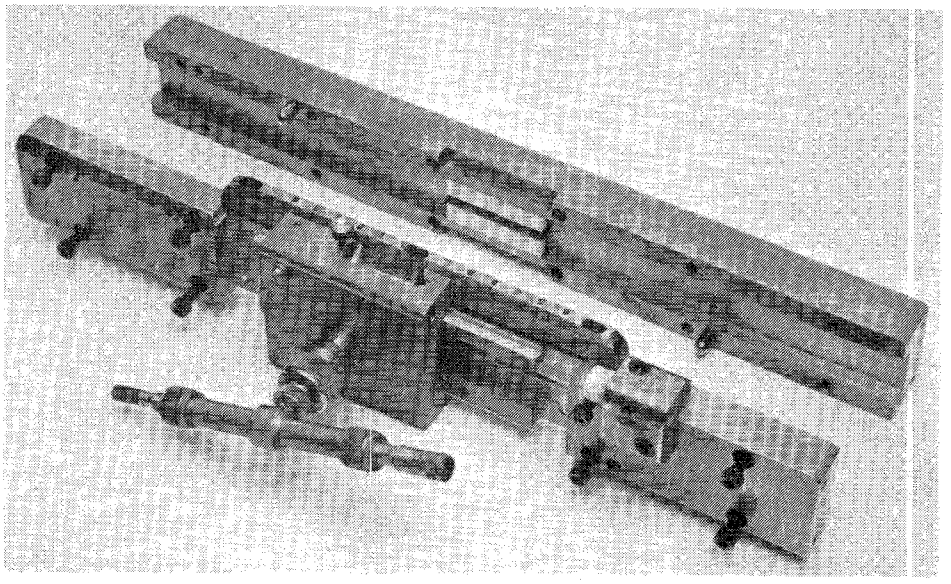

Fig. 5. Photograph of the two parts of the measurement section.

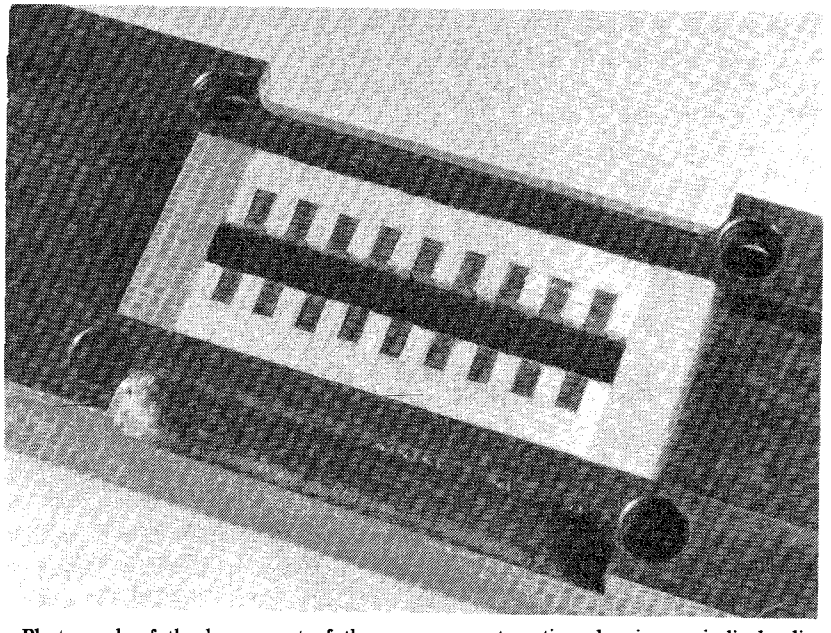

Fig. 6. Photograph of the lower part of the measurement section showing periodic loading of the ferrite-loaded waveguide.

without the wire. The type of ferrite used is TT1-390 and its properties are given in Table I. In the frequency range of interest, the losses due to the ferrite were found to be small and have been neglected in the investigation.

Periodic loading of this configuration was accomplished by weaving aluminum foil through and filling thin slots cut at regular intervals in the dielectric spacers, as shown in the photograph of Fig. 6. The thickness of the slot was 0.15 mm and its width was one half of that of the dielectric spacers. The foil made good contact with the top and bottom of the waveguide. Rather crude dielectric matching sections were used to reduce the reflections between the ferrite-loaded and air-filled waveguides.

In the upper part of the measurement section a slot was cut to allow insertion of capacitive probe to sample the electric field at 0.30 mm above the top face of the ferrite.

TABLE I
CHARACTERISTICS OF FERRITE

Type	TT 1-390
Material Composition	Magnesium, Manganese
Relative Permittivity, ϵ_f(9.4 GHz)	12.7 ±5%
Dielectric Loss Tangent (9.4 GHz)	<.00025
Saturation Magnetization ($4\pi M_s$)	2150 ±5% gauss @ 23°C

A cross section of the measurement section illustrating the slot and the probe is shown in Fig. 7. It was ascertained that the probe had little effect on the fields and that

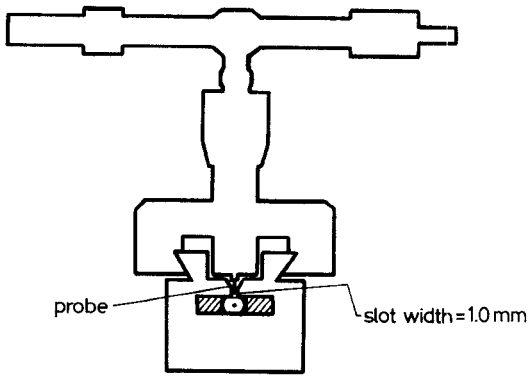

Fig. 7. Cross section of measurement section illustrating slot and probe.

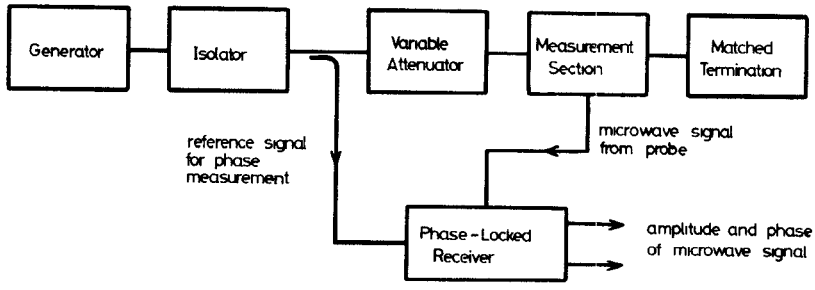

Fig. 8. Experimental arrangement for phase and amplitude measurements.

radiation from the slot was negligible. The probe was secured in a brass carriage which allows a travel of 7.5 cm. The microwave signal from the probe was fed into a phase-locked receiver where the magnitude and phase of the signal are measured.

B. Fields in Nonreciprocal Waveguides

A block diagram of the experimental arrangement for measuring the fields in the nonreciprocal section is shown in Fig. 8. The following two cases were investigated at the frequency of 9.0 GHz;

1) no periodic loading with the ferrite rod magnetized and unmagnetized; and
2) periodic loading by "inductive" diaphragms of spacing 0.22 cm with the ferrite rod magnetized and unmagnetized.

The scale reference for the field plots was established as shown in Fig. 9. The zero point for the probe displacement is taken as the point where the probe is directly over the interface nearest the generator. Thus, the positive values correspond to displacement of the probe towards the matched termination.

The field plots for case 1, no periodic loading, are shown in Fig. 10. For this particular case the crude matching sections were not present. The magnitude plot for unmagnetized ferrite is shifted upward for clarity. The standing wave patterns for magnetized ferrite are essentially the same for both directions of magnetization. Their periodicity is slightly different from that for unmagnetized ferrite.

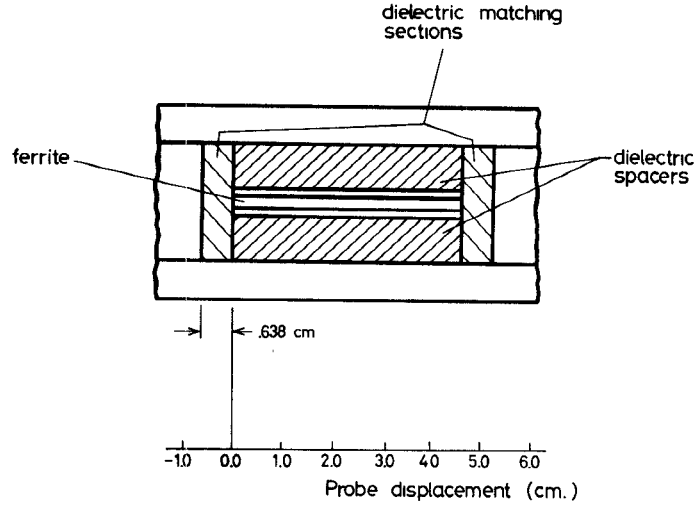

Fig. 9. Scale reference for phase and amplitude measurements.

The phase plots show clearly the three situations; the ferrite rod magnetized in opposite senses and the unmagnetized ferrite rod.

The field plots for the periodic structure are shown in Fig. 11. The magnitude plots for the two magnetizations are seen to be slightly shifted relative to each other. The periodicity of the standing wave patterns is different from that for unmagnetized ferrite. For both the reciprocal and nonreciprocal periodic structures the higher order Floquet harmonics appear to contribute little to the field structure. The phase plots show considerably less ripple due to the presence of the crude matching sections.

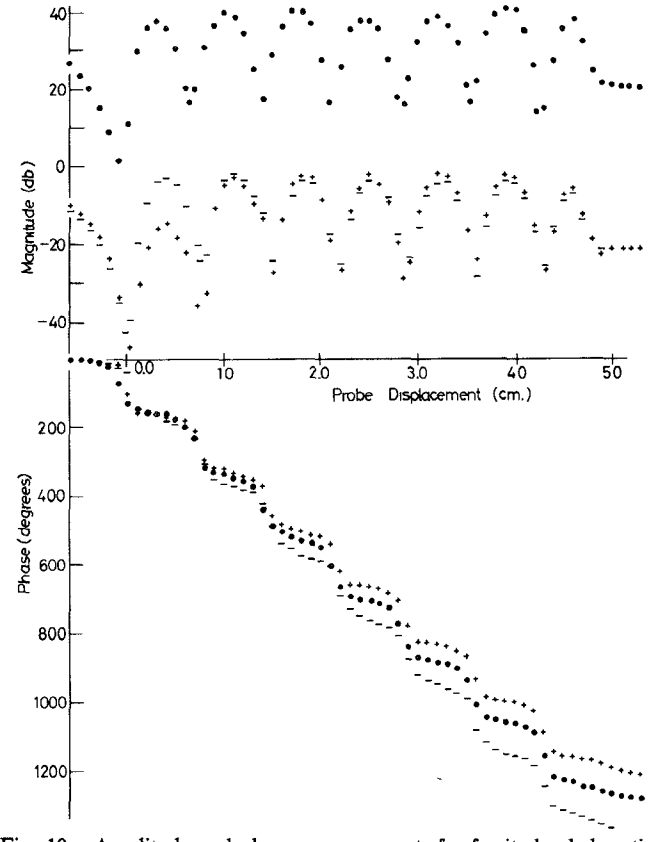

Fig. 10. Amplitude and phase measurements for ferrite loaded section without periodic loading. The points "+" and "−" correspond to magnetized ferrite and "•" to unmangetized ferrite.

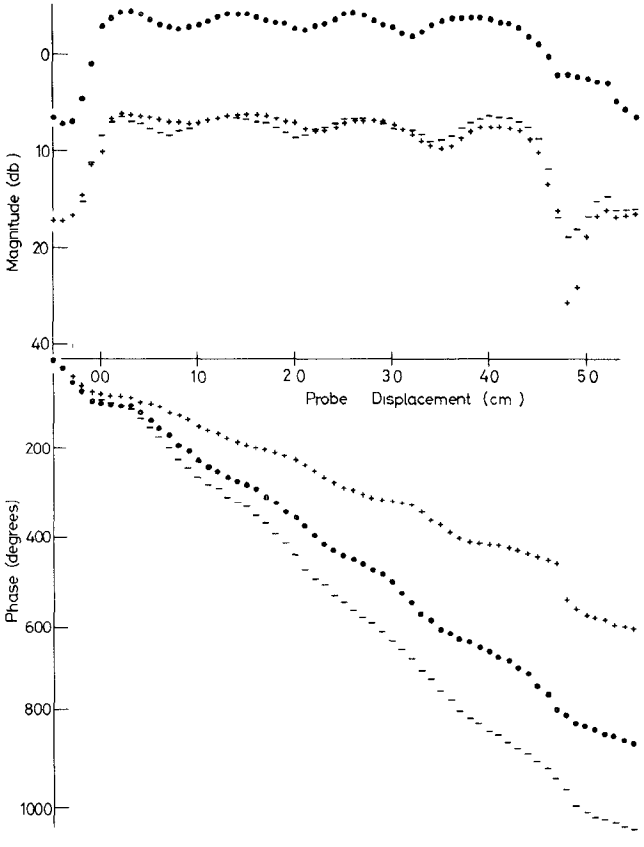

Fig. 11. Amplitude and phase measurements for ferrite-loaded section with periodic loading; spacing of diaphragms is 0.22 cm. The points "+" and "−" correspond to magnetized ferrite and "•" to unmagnetized ferrite.

The information in these plots may be interpreted by modelling the ferrite-loaded section of waveguide by a transmission line equivalent circuit. The total field is expressed as

$$E = A\exp(-j\beta^{+}z) + B\exp(j\beta^{-}z) \tag{18}$$

where the first term is the forward propagating mode and the second term is the reflected mode. The constants A and B depend on the properties of the medium and the interface effects. The magnitude of the total field is given by

$$|E| = |A||1 + \frac{B}{A}\exp[j(\beta^{+} + \beta^{-})z]| \tag{19}$$

and phase by

$$\arg(E) = \arg(A) - \beta^{+}z + \arg\left(1 + \frac{B}{A}\exp[j(\beta^{+} + \beta^{-})z]\right). \tag{20}$$

In the standing-wave pattern the distance between the minima is given by π/β_{av} where $\beta_{av} = (\beta^{+} + \beta^{-})/2$. The phase variation along the section consists of a linear term $\beta^{+}z$ and an oscillatory term $\arg(1 + B/A\exp[j(\beta^{+} + \beta^{-})z]$. The slope of the phase plot yields the propagation constant β^{+} of the forward propagating wave. In practice, greater accuracy of the slope measurement is obtained if the coefficient B is small.

For a nonreciprocal periodic structure

$$E = A\exp(-j\beta^{+}z) + B\exp(j\beta^{-}z)$$

corresponds to forward and reflected Bloch waves.

Measuring the slope of the phase change across the ferrite-loaded section of the waveguide provided an easy means of obtaining the propagation constant of the forward propagating wave. The crude dielectric matching sections helped to increase the accuracy of the measurements. As a check, the periodicities of the standing wave pattern were compared with those calculated from the propagation constants found using this method and were found to be in agreement.

To illustrate the effects of periodic loading clearly, a comparison of the phase variation along the ferrite loaded section of waveguide for no loading and for periodic loading is shown in Fig. 12. Two important points are noteworthy:

1) the phase change over the length of the section for both cases of magnetized and unmagnetized ferrite is reduced with periodic loading, as would be expected from the inductive nature of the loading; and
2) for the magnetized ferrite, the differential phase shift is substantially increased with periodic loading, thus agreeing with the findings of Spaulding [2], [3] and Kharadly [4].

C. Measurement of the Scattering Parameters of a Diaphragm in a Nonreciprocal Waveguide

The experimental arrangement for measuring the scattering parameters of a diaphragm is shown in Fig. 13. The interfaces between the ferrite-loaded and empty waveguides were matched using the crude dielectric matching sections as well as additional tuning elements.

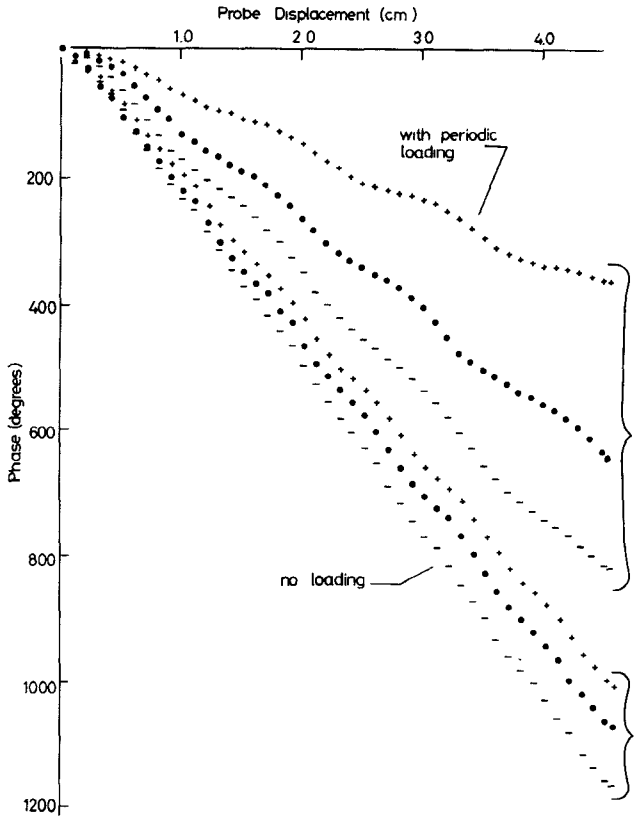

Fig. 12. Comparison of phase change across ferrite-loaded section between no loading and periodic loading; spacing of diaphragms is 0.22 cm.

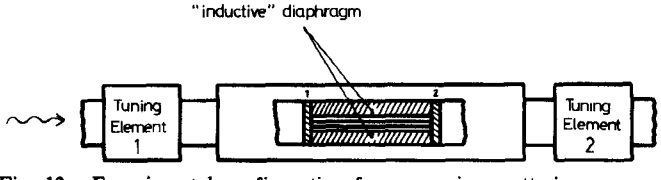

Fig. 13. Experimental configuration for measuring scattering parameters of diaphragm in ferrite-loaded waveguide.

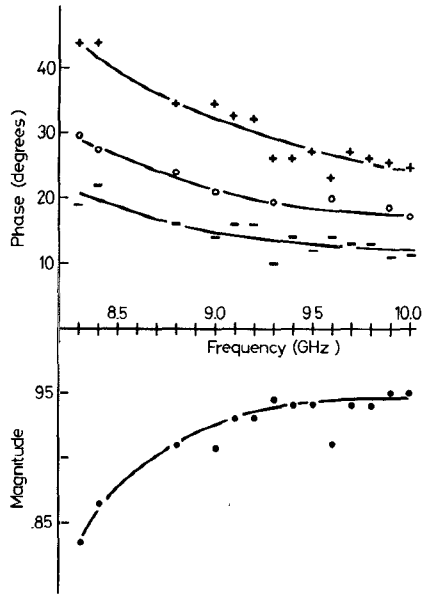

Fig. 14. Transmission coefficients for "inductive" diaphragm. For phase results the points "+" and "−" correspond to magnetized ferrite and "o" to unmagnetized ferrite. In the magnitude plot, results are given for maugetized ferrite and are independent of the direction of propagation.

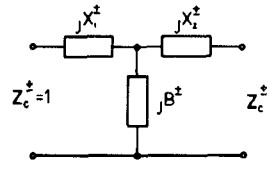

Fig. 15. Equivalent circuit for diaphragm in nonreciprocal waveguide.

After matching the interfaces, the scattering parameters of the diaphragm were obtained from the reflection and transmission coefficients of the ferrite-loaded section with the diaphragm in place. The reference points for the transmission measurements were obtained with the diaphragm removed. The transmission measurements were done using the null method in a bridge arrangement. The reflection measurements were used to verify that the angle of the reflection coefficient was indeed independent of direction of propagation (or magnetization) as predicted by mode-matching solutions [5].

The interfaces were matched in the following manner. With the wave incident as shown in Fig. 13, tuning element 2 was adjusted until the standing wave pattern measured in the ferrite-loaded section of waveguide was minimized. Interface 1 was then matched by adjusting tuning element 1.

In order to gain confidence in the accuracy of this method, the scattering parameters of the diaphragm were first measured with the ferrite unmagnetized. In this case the equivalent circuit for the diaphragm is a simple shunt susceptance and can be determined from either the magnitude or the phase of the transmission coefficient. Both quantities were measured and yielded consistent results. The transmission coefficients for the diaphragm with the ferrite magnetized were then measured. The experimental results are shown in Fig. 14 over the frequency of 8.3 to 9.9 GHz. Smooth curves are fitted to the experimental points. The experimental points, especially those for the phase measurements, appear to oscillate slightly about the curves. This is probably due to small reflections from the ferrite–air interfaces. The ferrite was magnetized such that the propagation constant of the forward-travelling wave was less than that of the backward-travelling wave. The results show that the transmission angle for the discontinuity is larger for the forward direction of propagation, as may be expected intuitively.

The discontinuity is now represented by the equivalent three element circuit of Fig. 15, where the elements have two sets of values corresponding to each direction of propagation (or magnetization). The characteristic impedance of the nonreciprocal transmission line $Z_c^{\pm}$ is set to 1. For the unmagnetized ferrite, the circuit simplifies to the shunt elements with $B^+ = B^-$. The circuit parameters are calculated from the smooth curves of Fig. 14 and are shown in Fig. 16. The dominant parameters for the nonreciprocal discontinuity are the shunt susceptances and these behave in a manner similar to that obtained in the reciprocal case. The series elements for the magnetized

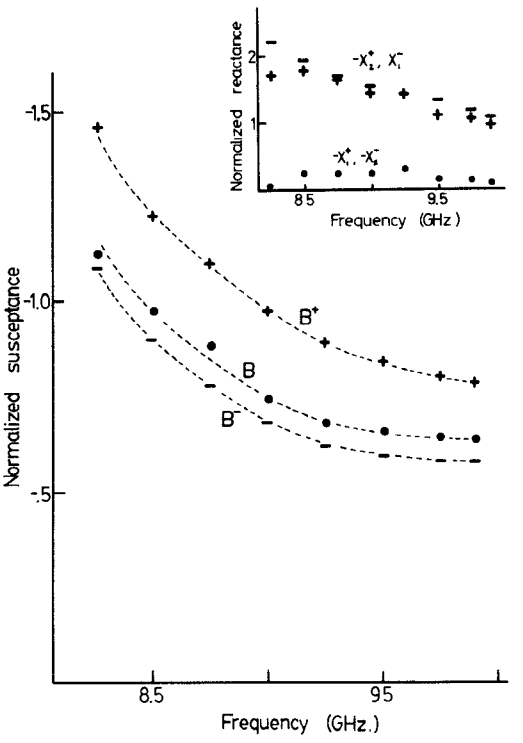

Fig. 16. Experimental results for circuit parameters of "inductive" diaphragm, calculated from the curves of Fig. 14.

TABLE II
PROPAGATION CONSTANTS

Frequency (GHz)	β_o^+ (rad/cm)	β_o (rad/cm)	β_o^- (rad/cm)
9.0	4.02	4.11	4.71
9.3	4.24	4.41	4.91
9.6	4.45	4.66	5.12
9.9	4.68	4.94	5.40

case are relatively small. The experimental points for X_1^+, X_1^- are too small to plot individually and lie within the solid dots.

D. Measurement on Nonreciprocal Periodic Structures

Periodic structures were constructed with spacings ranging from 0.22 cm to 0.51 cm. The measurements were carried out at four frequencies 9.0 GHz, 9.3 GHz, 9.6 GHz, and 9.9 GHz with the ferrite magnetized and unmagnetized.

The propagation constants of the ferrite-loaded section with no periodic loading were first measured at these frequencies using the method described in Section III-B and are shown in Table II. With these measurements and the scattering parameters of the "inductive" diaphragm, found as described in Section III-C, the variation of the propagation constants with frequency for the periodic structures was calculated. These calculations are represented by the solid curves in Fig. 17 (a)–(d). The measurements on these structures are represented by the points in these figures. The agreement is seen to be better at the higher frequencies and for the larger spacings. As the frequency and spacing decrease, the discrepancy between the experimental and theoretical values increases, and it appears that the effects of higher mode interaction between the diaphragms become more important. Higher mode interaction could be accounted for by increasing the dimensions of the wave matrix to include the modes which appreciably interact. In practice, however, it would be difficult to determine all the matrix elements.

Finally, the differential change in the propagation constants is plotted as a function of the inverse of the spacing between the loading elements, Fig. 18. The solid line is theoretically obtained by using the measured scattering parameters of the diaphragm. It is clear that the differential change in the propagation constant is significantly

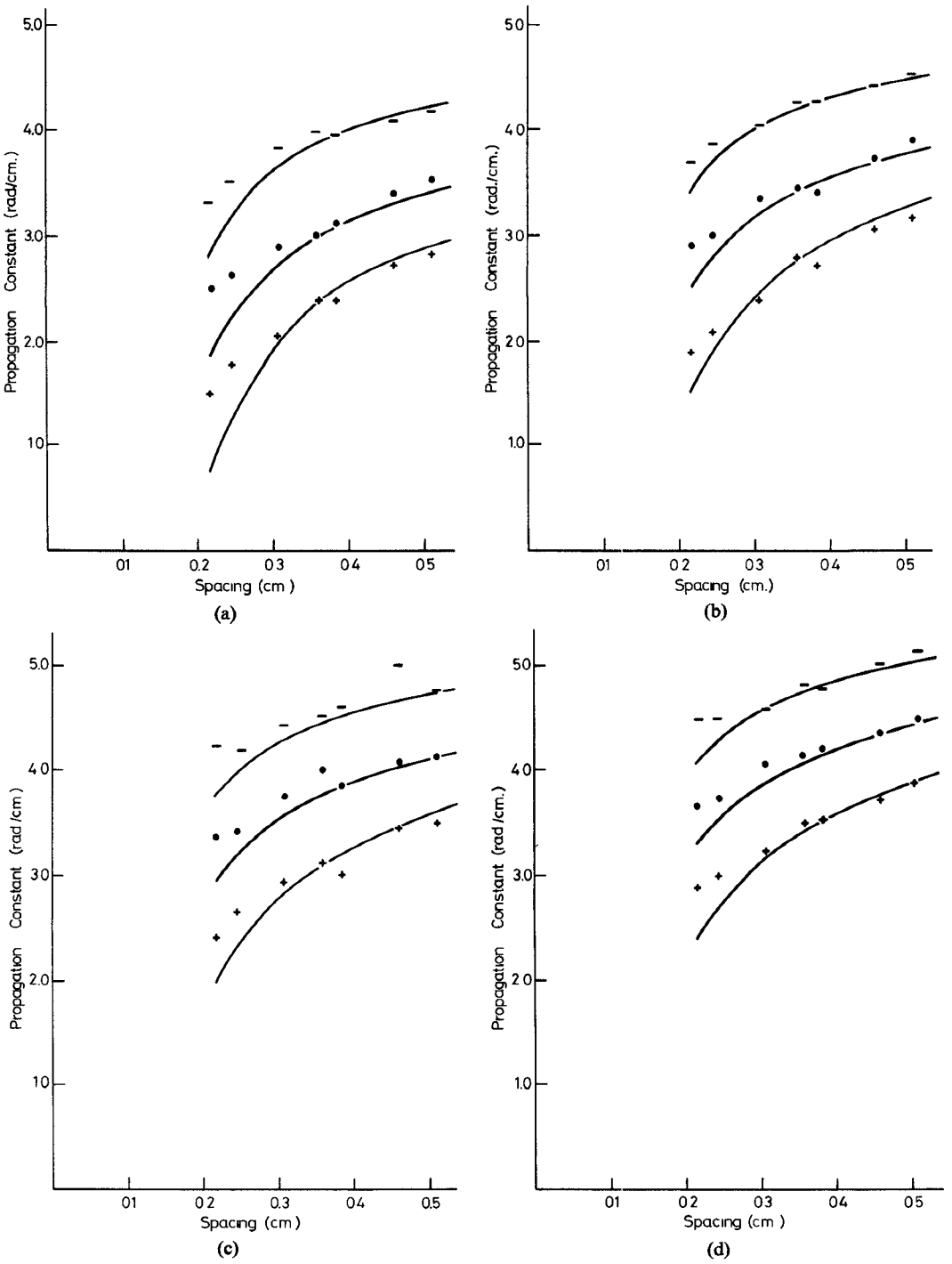

Fig. 17. Measurement of periodic structures with the predicted values indicated by the solid curves. (a) freq. = 9.0 GHz. (b) freq. = 9.3 GHz. (c) freq. = 9.6 GHz. (d) freq. = 9.9 GHz.

increased using periodic loading. For the smallest spacing used this increase is approximately 2.6 times that for no periodic loading.

V. Conclusions

An experimental investigation has been made of a certain type of nonreciprocal periodic structure. Periodic loading was accomplished through regular placement of thin "inductive" diaphragms. This type of loading is easy to implement and provides significant improvement in the differential phase shift characteristics and could be of special interest in the design of nonreciprocal ferrite phase shifters.

The main contributions in this work may be summarized as follows:

1) The wave transmission line approach has been shown to be applicable for the analysis of nonreciprocal

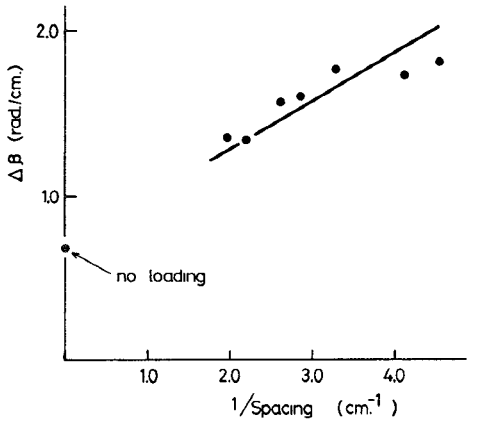

Fig. 18. Differential phase shift per unit length as a function of the spacing of the periodic structure.

periodic structures where the periodic loading is accomplished through regular placement of thin obstacles. The values of the propagation constants obtained experimentally agree quite well with those predicted analytically (using measured values of the scattering parameters) except for the smaller spacings between the loading elements. The discrepancy at these spacings is attributed to higher mode interaction, which was not included in this analysis. The effect of the higher mode interaction appears to be of the same order for both reciprocal and nonreciprocal periodic structures.

2) A direct experimental method has been used to measure the magnitude and phase of the electric field along a ferrite-loaded section of waveguide. This is achieved through the use of a specially constructed slotted section. The slope of the phase variation thus obtained yields directly the propagation constant of the forward propagating wave. It also clearly illustrates the effect of periodic loading on the differential phase shift. The magnitude plots indicate only a slight dependence on the direction of magnetization and no apparent contribution from the higher order Floquet harmonics to the field structure of the periodic structures investigated.

3) The scattering parameters of an "inductive" diaphragm were measured accurately and were used to derive a three-element equivalent circuit. It is shown that for the magnetized ferrite, the nonreciprocal nature of the discontinuity is reflected mainly in the values of the shunt susceptances. The series reactive elements are relatively small but are necessary to satisfy the unitary conditions of the scattering matrix of the discontinuity.

References

[1] C. Elachi, "Waves in active and passive periodic structures: A review," *Proc. IEEE*, vol. 64, pp. 1666–1698, Dec. 1976.

[2] W. G. Spaulding, "A periodic loaded, latching, nonreciprocal ferrite phase shifter," presented at the IEEE G-MTT Int. Microwave Symp., Dallas, TX, 1969.

[3] W. G. Spaulding, "The application of periodic loading to a ferrite phase shifter design," *IEEE Trans. Microwave Theory Tech.*, vol. MTT-19 pp. 922–928, Dec. 1971.

[4] M. M. Z. Kharadly, "Periodically loaded nonreciprocal transmission lines for phase shifter applications," *IEEE Trans. Microwave Theory Tech.*, vol. MTT-22, pp. 635–640, June 1974.

[5] T. A. Enegren and M. M. Z. Kharadly, "Transverse discontinuities in nonreciprocal waveguides," *IEEE Trans. Microwave Theory Tech.*, to be published.

[6] F. J. Bernues and B. M. Bolle, "The ferrite-loaded waveguide discontinuity problem," *IEEE Trans. Microwave Theory Tech.*, vol. MTT-22, pp. 1187–1193, Dec. 1974.

[7] W. K. McRitchie and M. M. Z. Kharadly, "Numerical solution for nonreciprocal inhomogeneous waveguide interface," *Proc. IEE*, vol. 123, pp. 391–393, 1976.